Supplemental Data

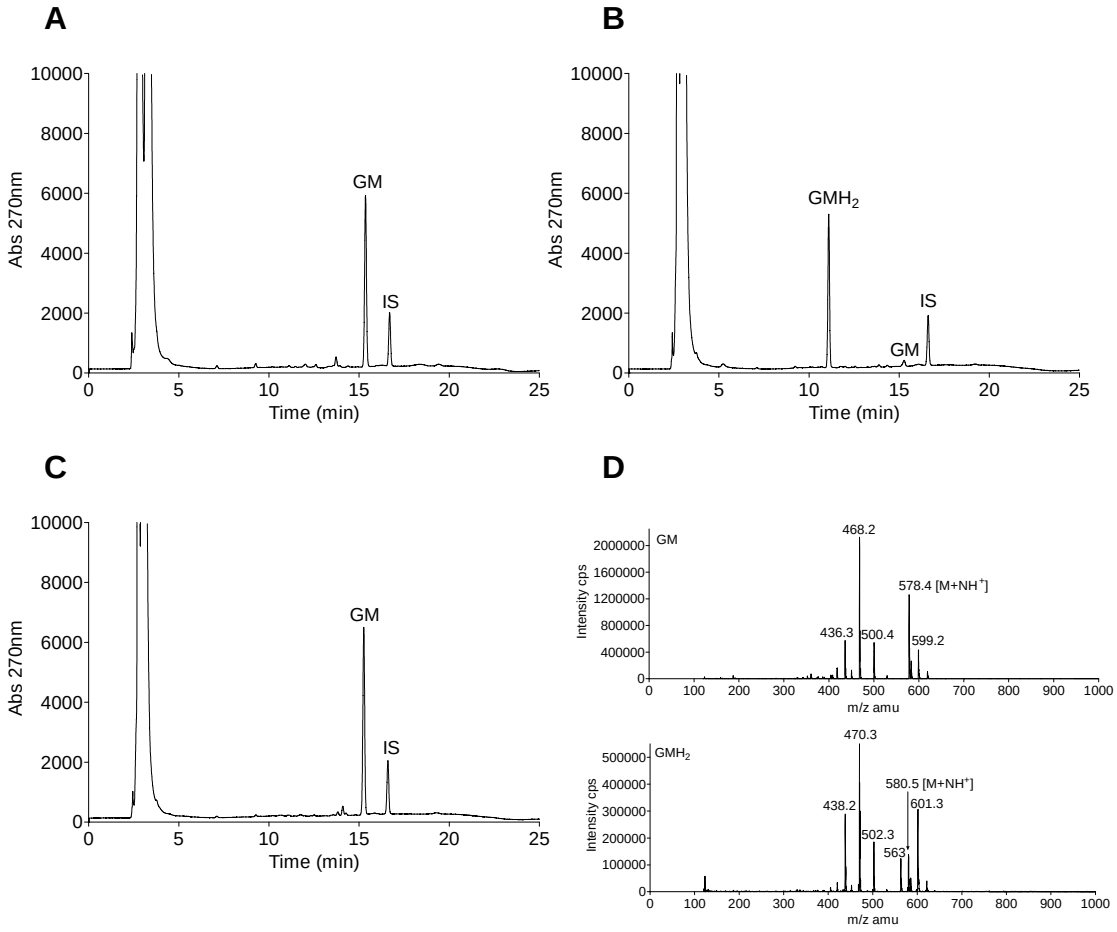

Figure 1.2. HPLC and LC-MS analysis of the reduction of GM by NQO1 to GMH_2.
HPLC analysis of the rhNQO1-mediated reduction of (A) GM to (B) GMH_2 and inhibition of this reduction by (C) ES936. (A) GM and NADH; (B) GM, NADH, and rhNQO1; (C) GM, NADH, rhNQO1, and ES936 (1 µmol/L). Reaction conditions: 20 µmol/L GM, 500 µmol/L NADH, and 6.6 µg rhNQO1 in 50 mmol/L potassium phosphate buffer (pH 7.4; 1 mL) containing 1 mg/mL BSA. After 30 minutes, the internal standard N-phenyl-1-naphthylamine (10 µg/mL) was added, the sample centrifuged and the supernatant was analyzed immediately by HPLC at 270 nm. (D) LC-MS confirmed GMH_2 as the product of NQO1-mediated reduction of GM.

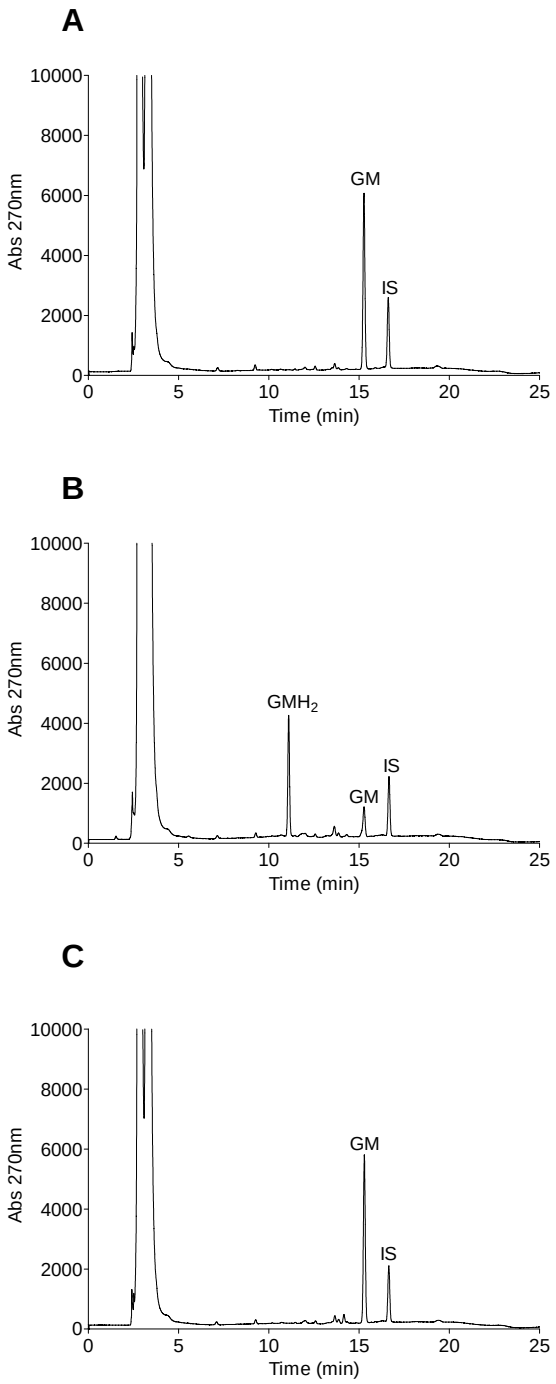

Figure 3.2. HPLC analysis of GMH_2 formation by MDA468 and MDA468/NQ16 cell sonicates.
HPLC analysis confirmed the formation of GMH_2 following reduction of GM by MDA468/NQ16 cell sonicates. (A) GM, NADH, and MDA468 cell sonicates; (B) GM, NADH, and MDA468/NQ16 cell sonicates; (C) GM, NADH, and MDA468/NQ16 cell sonicates and ES936 (1 μmol/L). Reaction conditions: 20 μmol/L GM, 500 μmol/L NADH, and 500 μg of cell sonicate in 50 mmol/L potassium phosphate buffer (pH 7.4; 1 mL) containing 1 mg/mL BSA. After 30 minutes, the internal standard N-phenyl-1-naphthylamine (10 μg/mL) was added, the sample centrifuged and the supernatant was analyzed immediately by HPLC at 270 nm.

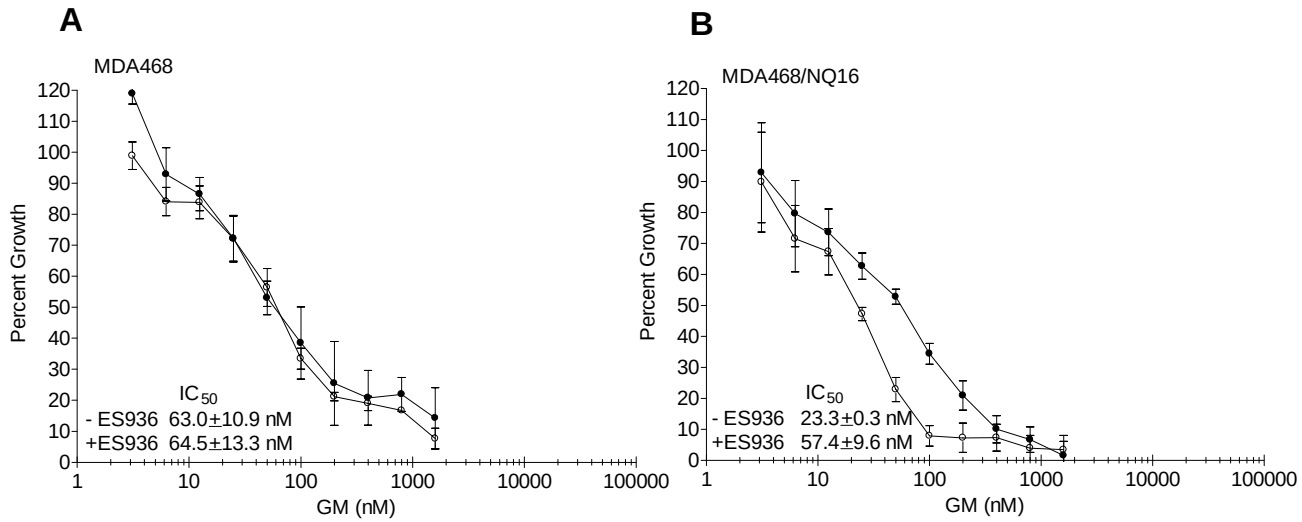

Figure 4.2. Effect of GM on growth inhibition and Hsp90 client proteins in human breast cancer cells. Growth inhibition following GM treatment was measured by MTT analysis in (A) MDA468 (NQO1-null) and (B) MDA468/NQ16 (high NQO1) cell lines in the presence (filled symbols) and absence (open symbols) of ES936. Points, mean (n = 3); bars, SD.

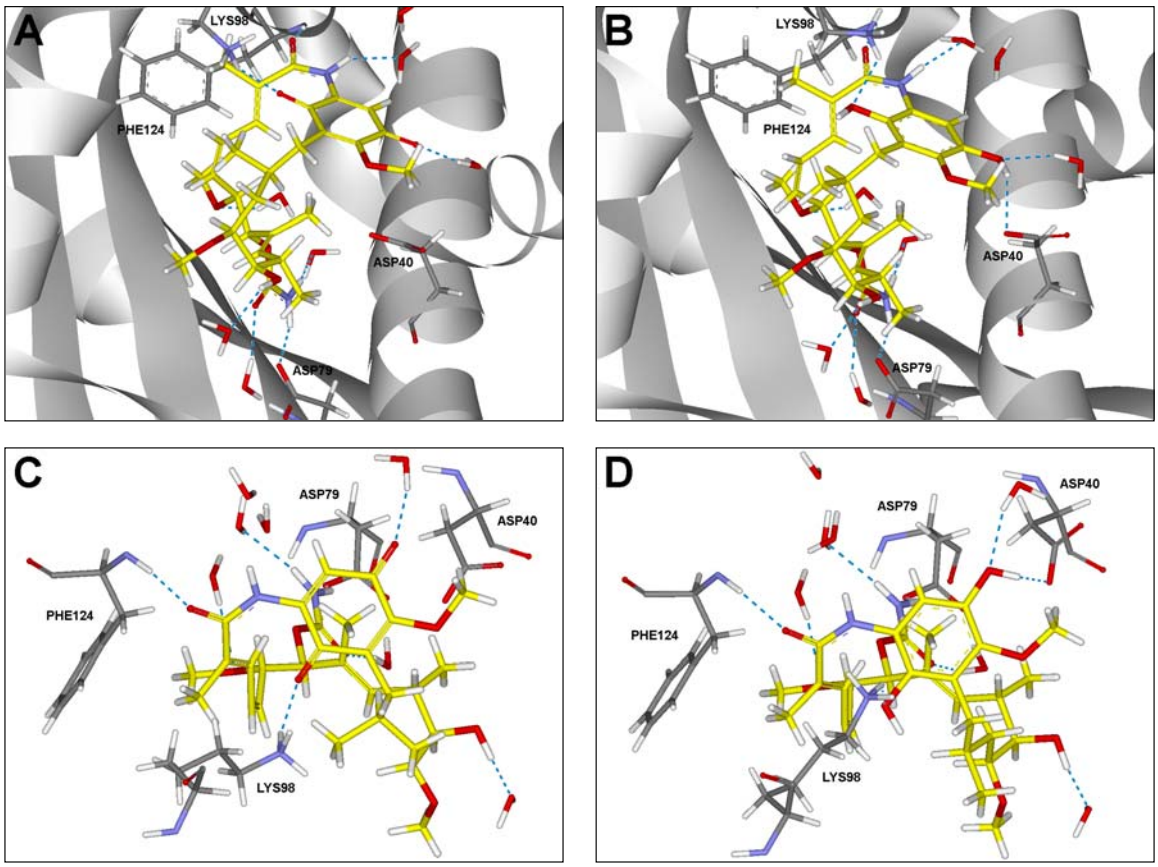

Figure 5.2. Molecular modeling of the N-terminal of the yeast Hsp90-GM/GMH_2 complex.
Flat ribbon representation of the yeast Hsp90 ATP-binding domain with (A) GM and (B) GMH_2 and stick display style representation of the key interactions with (C) GM and (D) GM all figures display hydrogen bond contacts (blue dashed lines) with amino acid residues and water molecules (colored by atom type, except ligand carbons atoms which are colored yellow). The figures were constructed using Discovery Studio Viewer Professional Software (Accelrys, Inc., San Diego, CA).

Compound	E_{vdw} (kcal/mol)	E_{elect} (kcal/mol)	E_{total} (kcal/mol)	H-Bond Interaction		H-Bond Distance (Å)
				Amino Acid / Solvent	Ligand	
GDM	-37.9	-13.0	-50.9	ASP-79	Carbamate NH_2	1.99
				LYS+98	Quinone C=O	2.02
				PHE124	Amide C=O	2.09
				HOH400	Carbamate C=O	2.06
				HOH402	Carbamate NH_2	2.27
				HOH403	Methoxy (ansa) OCH_3	2.29
				HOH405	Hydroxy (ansa) OH	2.08
				HOH407	Quinone C=O	1.93
				HOH528	Amide NH	2.18
$GDMH_2$	-37.0	-33.8	-70.7	ASP-40	Hydroquinone O-H	2.15
				ASP-79	Carbamate NH_2	2.06
				LYS+98	Hydroquinone C-O	2.16
				PHE124	Amide C=O	2.49
				HOH400	Carbamate C=O	2.25
				HOH402	Carbamate NH_2	2.24
				HOH403	Methoxy (ansa) OCH_3	2.31
				HOH403	Carbamate R-O-$CONH_2$	2.50
				HOH405	Hydroxy (ansa) OH	2.04
				HOH407	Hydroquinone O-H	2.04
				HOH529	Amide NH	2.05

Table 2.2. Total interaction energy, van der Waals, electrostatic energy, and hydrogen bonding interactions between yeast Hsp90 and GM/GMH_2.

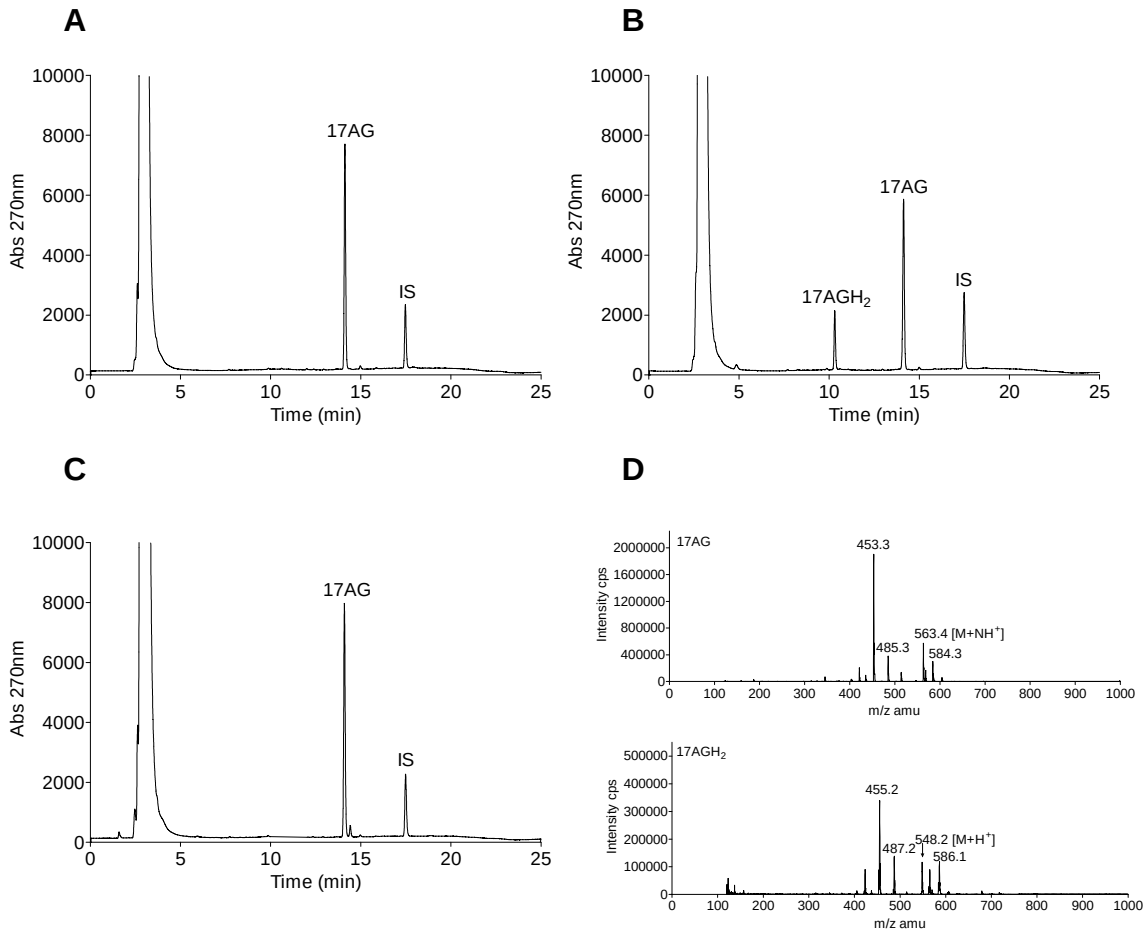

Figure 1.3. HPLC and LC-MS analysis of the reduction of 17AG by NQO1 to $17AGH_2$.
HPLC analysis of the rhNQO1-mediated reduction of (A) 17AG to (B) $17AGH_2$ and inhibition of this reduction by (C) ES936. (A) 17AG and NADH; (B) 17AG, NADH, and rhNQO1; (C) 17AG, NADH, rhNQO1, and ES936 (1 µmol/L). Reaction conditions: 20 µmol/L 17AG, 500 µmol/L NADH, and 6.6 µg rhNQO1 in 50 mmol/L potassium phosphate buffer (pH 7.4; 1 mL) containing 1 mg/mL BSA. After 30 minutes, the internal standard N-phenyl-1-naphthylamine (10 µg/mL) was added, the sample centrifuged and the supernatant was analyzed immediately by HPLC at 270 nm. (D) LC-MS confirmed $17AGH_2$ as the product of NQO1-mediated reduction of 17AG.

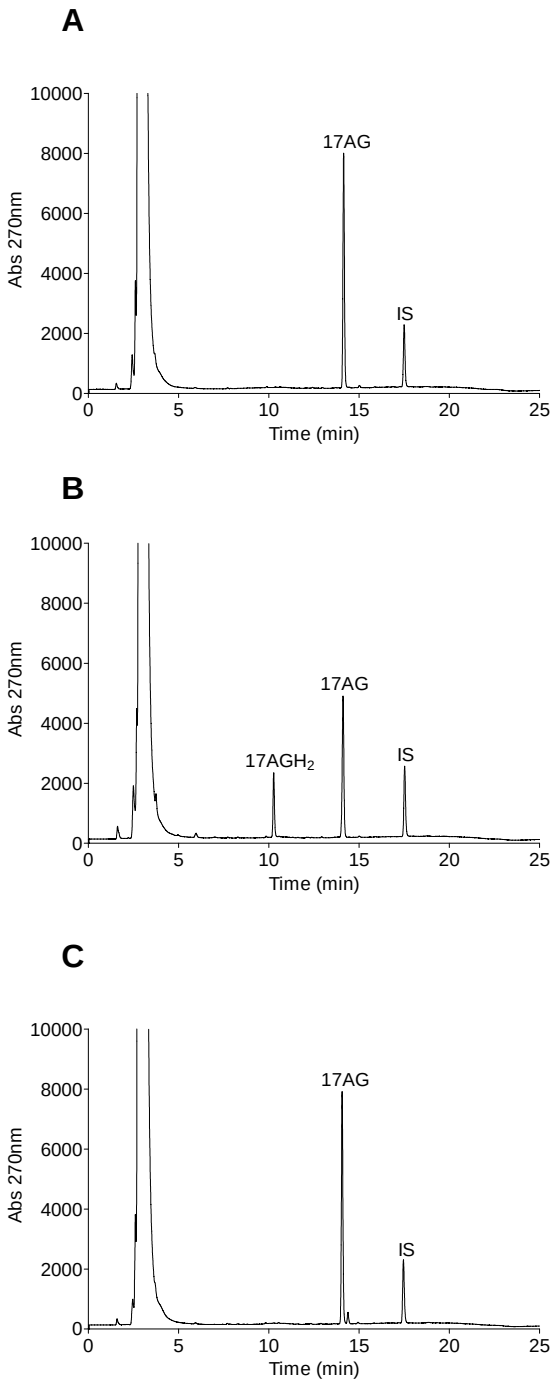

Figure 3.3. HPLC analysis of $17AGH_2$ formation by MDA468 and MDA468/NQ16 cell sonicates.
HPLC analysis confirmed the formation of $17AGH_2$ following reduction of 17AG by MDA468/NQ16 cell sonicates. (A) 17AG, NADH, and MDA468 cell sonicates; (B) 17AG, NADH, and MDA468/NQ16 cell sonicates; (C) 17AG, NADH, and MDA468/NQ16 cell sonicates and ES936 (1 μmol/L). Reaction conditions: 20 μmol/L 17AG, 500 μmol/L NADH, and 1 mg of cell sonicate in 50 mmol/L potassium phosphate buffer (pH 7.4; 1 mL) containing 1 mg/mL BSA. After 30 minutes, the internal standard N-phenyl-1-naphthylamine (10 μg/mL) was added, the sample centrifuged and the supernatant was analyzed immediately by HPLC at 270 nm.

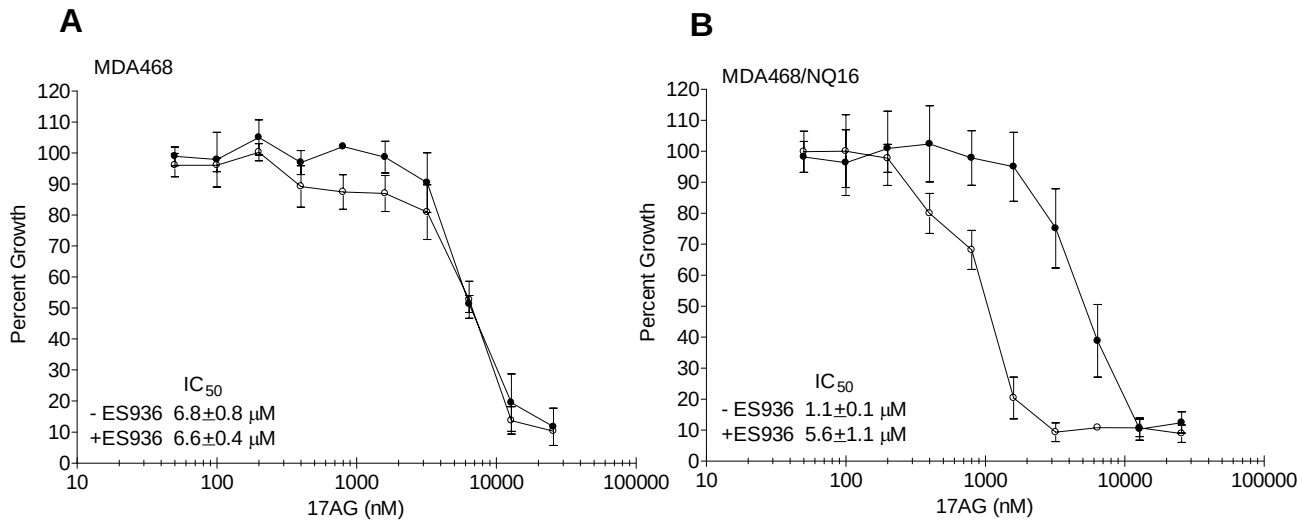

Figure 4.3. Effect of 17AG on growth inhibition and Hsp90 client proteins in human breast cancer cells. Growth inhibition following 17AG treatment was measured by MTT analysis in (A) MDA468 (NQO1-null) and (B) MDA468/NQ16 (high NQO1) cell lines in the presence (filled symbols) and absence (open symbols) of ES936. Points, mean (n = 3); bars, SD.

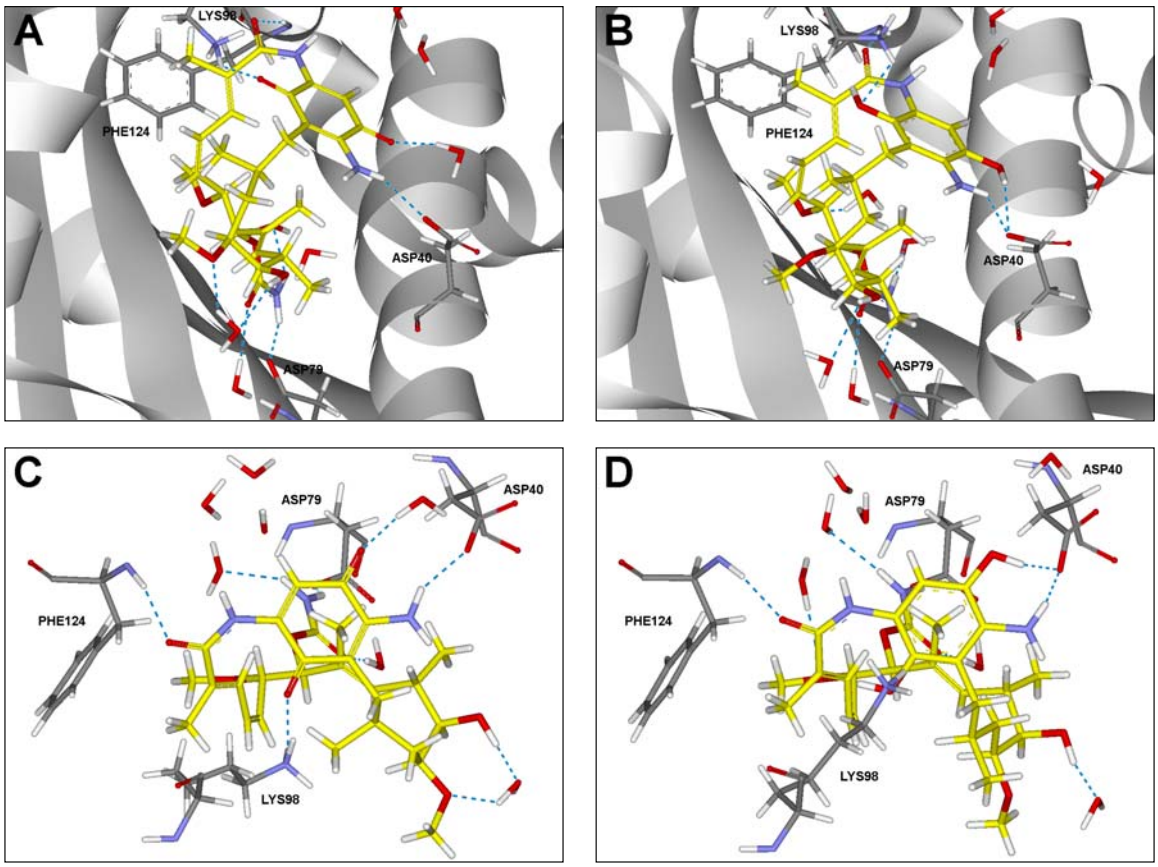

Figure 5.3. Molecular modeling of the N-terminal of the yeast Hsp90-17AG/17AGH$_2$ complex.
Flat ribbon representation of the yeast Hsp90 ATP-binding domain with (A) 17AG and (B) 17AGH$_2$ and stick display style representation of the key interactions with (C) 17AG and (D) 17AG all figures display hydrogen bond contacts (blue dashed lines) with amino acid residues and water molecules (colored by atom type, except ligand carbons atoms which are colored yellow). The figures were constructed using Discovery Studio Viewer Professional Software (Accelrys, Inc., San Diego, CA).

Compound	E_{vdw} (kcal/mol)	E_{elect} (kcal/mol)	E_{total} (kcal/mol)	H-Bond Interaction		H-Bond Distance (Å)
				Amino Acid / Solvent	Ligand	
17-AG	-29.5	-21.7	-51.2	ASP-40	Amine -NH_2	2.10
				ASP-79	Carbamate NH_2	1.96
				LYS+98	Quinone C=O	1.93
				PHE124	Amide C=O	2.42
				HOH400	Carbamate C=O	2.06
				HOH403	Carbamate NH_2	2.18
				HOH405	Hydroxy (ansa) OH	2.03
				HOH405	Methoxy (ansa) OCH_3	2.02
				HOH407	Quinone C=O	1.76
17-AGH_2	-35.0	-38.1	-73.0	ASP-40	Hydroquinone O-H	1.87
				ASP-40	Amine -NH_2	2.11
				ASP-79	Carbamate NH_2	2.02
				LYS+98	Hydroquinone C-O	2.44
				PHE124	Amide C=O	2.34
				HOH400	Carbamate C=O	2.00
				HOH402	Carbamate NH_2	2.27
				HOH403	Methoxy (ansa) OCH_3	2.38
				HOH405	Hydroxy (ansa) OH	2.38

Table 2.3. Total interaction energy, van der Waals, electrostatic energy, and hydrogen bonding interactions between yeast Hsp90 and 17AG/17AGH_2.

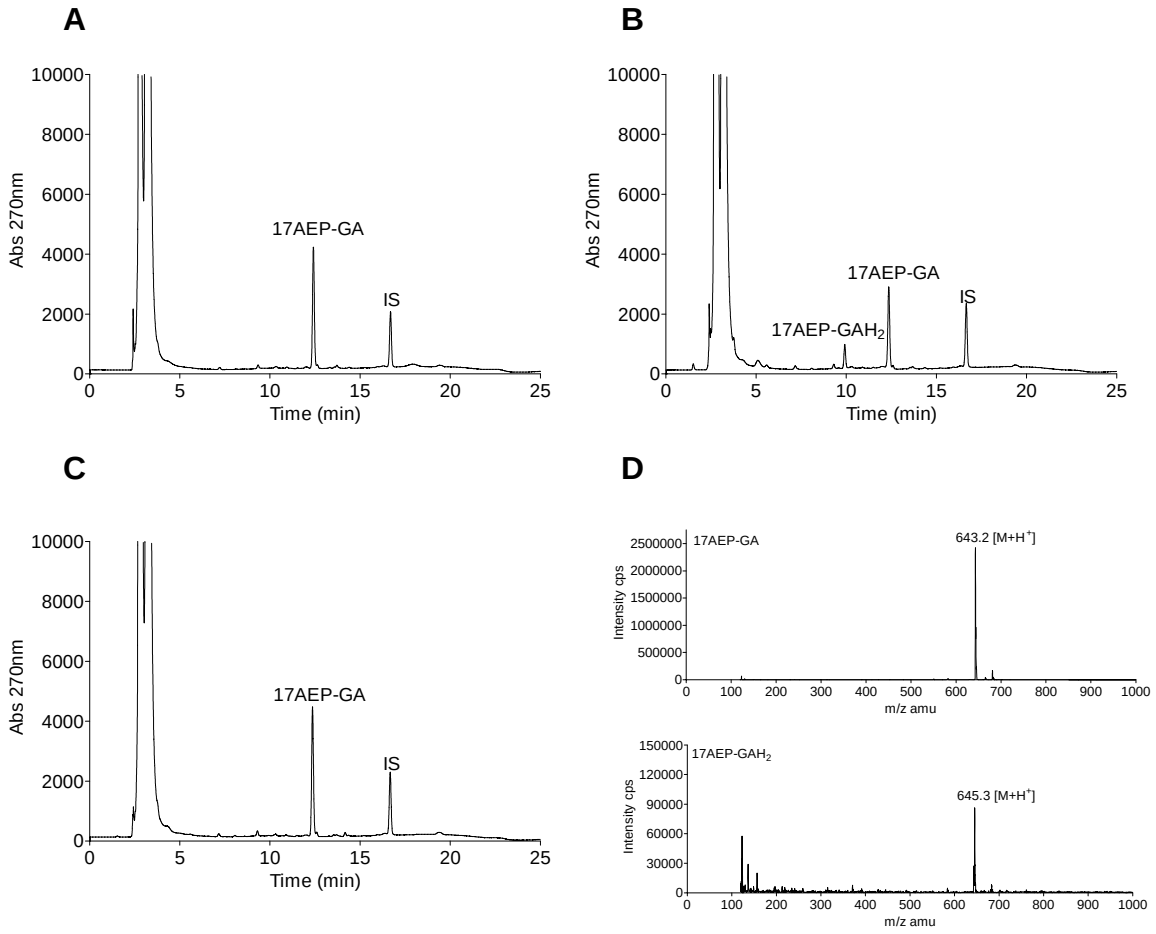

Figure 1.4. HPLC and LC-MS analysis of the reduction of 17AEP-GA by NQO1 to 17AEP-GAH$_2$.
HPLC analysis of the rhNQO1-mediated reduction of (A) 17AEP-GA to (B) 17AEP-GAH$_2$ and inhibition of this reduction by (C) ES936. (A) 17AEP-GA and NADH; (B) 17AEP-GA, NADH, and rhNQO1; (C) 17AEP-GA, NADH, rhNQO1, and ES936 (1 µmol/L). Reaction conditions: 20 µmol/L 17AEP-GA, 500 µmol/L NADH, and 16.5 µg rhNQO1 in 50 mmol/L potassium phosphate buffer (pH 7.4; 1 mL) containing 1 mg/mL BSA. After 30 minutes, the internal standard N-phenyl-1-naphthylamine (10 µg/mL) was added, the sample centrifuged and the supernatant was analyzed immediately by HPLC at 270 nm. (D) LC-MS confirmed 17AEP-GAH$_2$ as the product of NQO1-mediated reduction of 17AEP-GA.

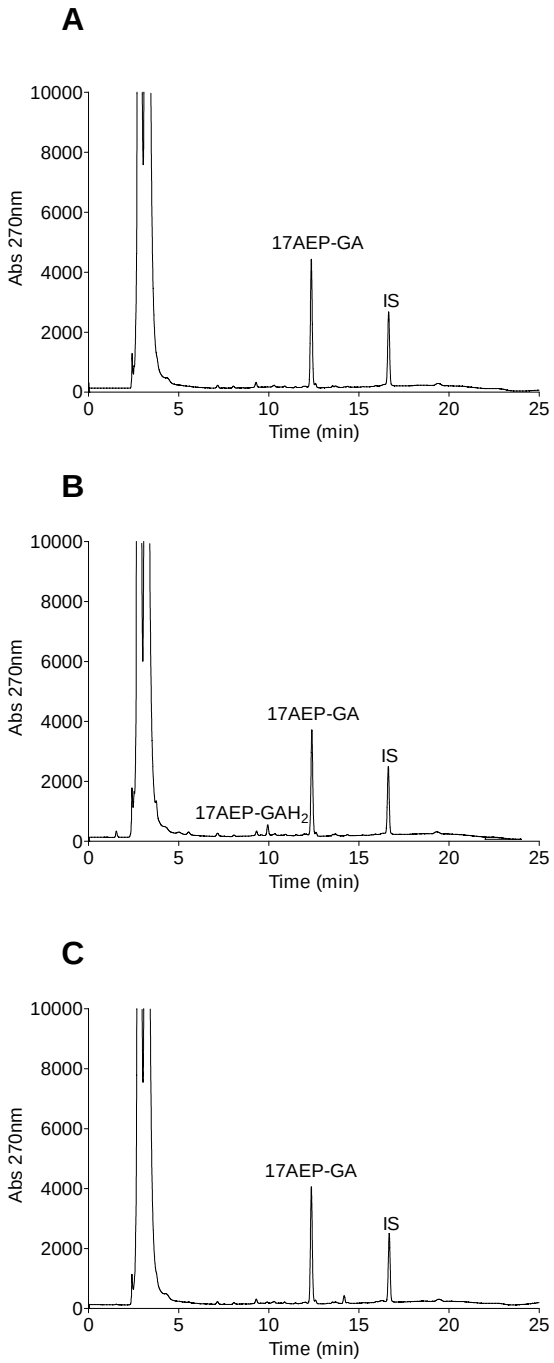

Figure 3.4. HPLC analysis of 17AEP-GAH$_2$ formation by MDA468 and MDA468/NQ16 cell sonicates. HPLC analysis confirmed the formation of 17AEP-GAH$_2$ following reduction of 17AEP-GA by MDA468/NQ16 cell sonicates. (A) 17AEP-GA, NADH, and MDA468 cell sonicates; (B) 17AEP-GA, NADH, and MDA468/NQ16 cell sonicates; (C) 17AEP-GA, NADH, and MDA468/NQ16 cell sonicates and ES936 (1 µmol/L). Reaction conditions: 20 µmol/L 17AEP-GA, 500 µmol/L NADH, and 2 mg of cell sonicate in 50 mmol/L potassium phosphate buffer (pH 7.4; 1 mL) containing 1 mg/mL BSA. After 30 minutes, the internal standard N-phenyl-1-naphthylamine (10 µg/mL) was added, the sample centrifuged and the supernatant was analyzed immediately by HPLC at 270 nm.

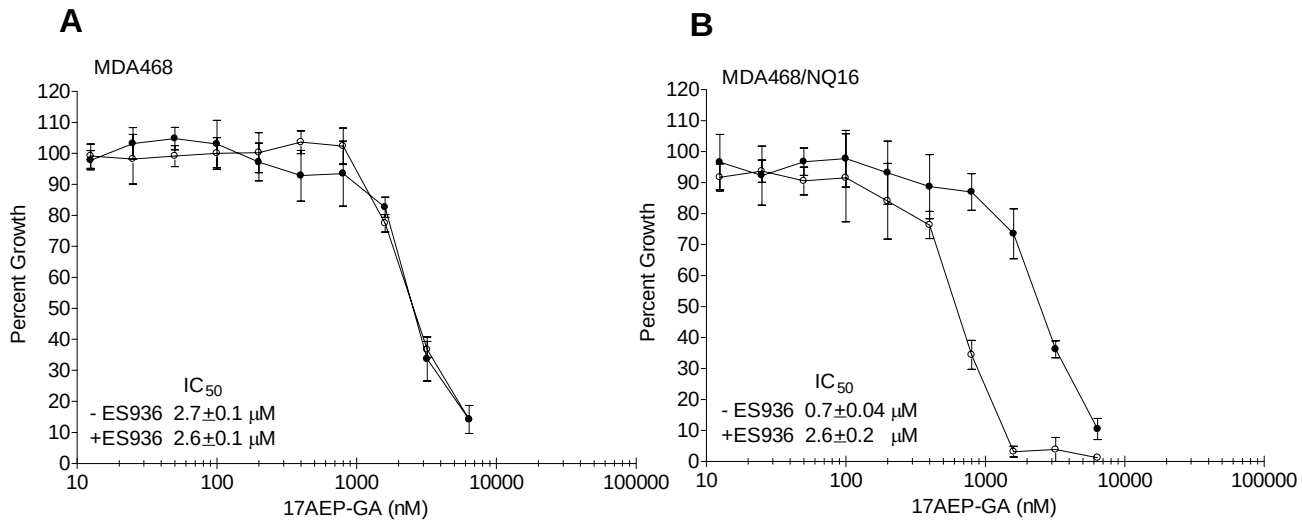

Figure 4.4. Effect of 17AEP-GA on growth inhibition and Hsp90 client proteins in human breast cancer cells.

Growth inhibition following 17AEP-GA treatment was measured by MTT analysis in (A) MDA468 (NQO1-null) and (B) MDA468/NQ16 (high NQO1) cell lines in the presence (filled symbols) and absence (open symbols) of ES936. Points, mean (n = 3); bars, SD.

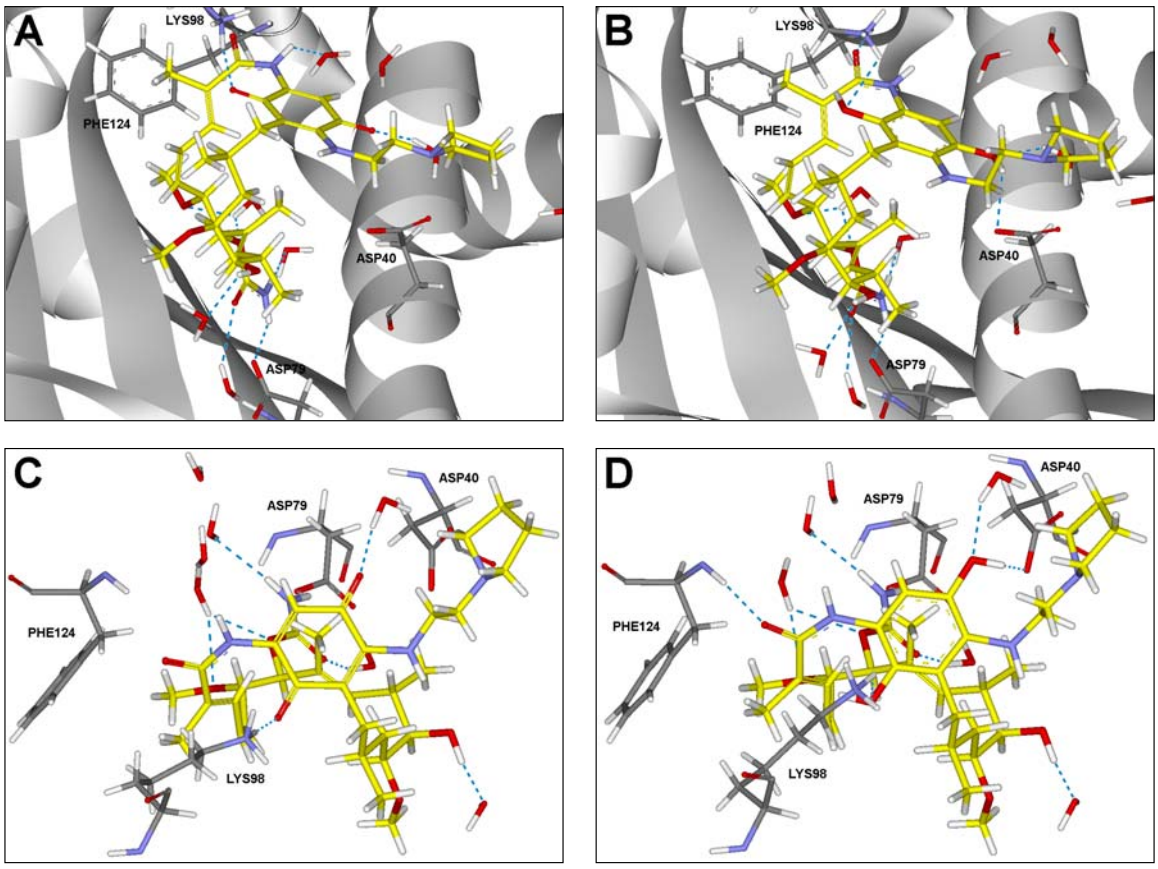

Figure 5.4. Molecular modeling of the N-terminal of the yeast Hsp90-17AEP-GA/17AEP-GAH$_2$ complex. Flat ribbon representation of the yeast Hsp90 ATP-binding domain with (A) 17AEP-GA and (B) 17AEP-GAH$_2$ and stick display style representation of the key interactions with (C) 17AEP-GA and (D) 17AEP-GA all figures display hydrogen bond contacts (blue dashed lines) with amino acid residues and water molecules (colored by atom type, except ligand carbons atoms which are colored yellow). The figures were constructed using Discovery Studio Viewer Professional Software (Accelrys, Inc., San Diego, CA).

Compound	E_{vdw} (kcal/mol)	E_{elect} (kcal/mol)	E_{total} (kcal/mol)	H-Bond Interaction		H-Bond Distance (Å)
				Amino Acid / Solvent	Ligand	
17-AEP-GA	-27.9	-24.8	-52.7	ASP-79	Carbamate NH_2	2.12
				LYS+98	Quinone C=O	1.66
				HOH400	Carbamate C=O	2.39
				HOH402	Carbamate NH_2	2.40
				HOH403	Methoxy (ansa) OCH_3	2.49
				HOH403	Carbamate R-O-$CONH_2$	2.20
				HOH405	Hydroxy (ansa) OH	2.08
				HOH407	Quinone C=O	1.69
				HOH529	Amide NH	2.13
17-AEP-GAH_2	-28.3	-27.6	-55.9	ASP-40	Hydroquinone O-H	2.24
				ASP-79	Carbamate NH_2	2.07
				LYS+98	Hydroquinone O-H	2.49
				PHE124	Amide C=O	1.91
				HOH400	Carbamate C=O	2.25
				HOH402	Carbamate NH_2	2.25
				HOH403	Methoxy (ansa) OCH_3	2.33
				HOH403	Carbamate R-O-$CONH_2$	2.43
				HOH405	Hydroxy (ansa) OH	2.14
				HOH407	Hydroquinone O-H	1.94

Table 2.4. Total interaction energy, van der Waals, electrostatic energy, and hydrogen bonding interactions between yeast Hsp90 and 17AEP-GA/17AEP-GAH_2.